DETECTION OF INTEGRINS USING SURFACE ENHANCED RAMAN SPECTROSCOPY

A Thesis

by

VIRGIL ALEXANDER GANT

Submitted to the Office of Graduate Studies of
Texas A&M University
in partial fulfillment of the requirements for the degree of

MASTER OF SCIENCE

May 2005

Major Subject: Biomedical Engineering

DETECTION OF INTEGRINS USING SURFACE ENHANCED RAMAN SPECTROSCOPY

A Thesis

by

VIRGIL ALEXANDER GANT

Submitted to Texas A&M University
in partial fulfillment of the requirements
for the degree of

MASTER OF SCIENCE

Approved as to style and content by:

Gerard L. Coté (Co-Chair of Committee)	Gerald A. Meininger (Co-Chair of Committee)
Lihong Wang (Member)	Gerard L. Coté (Head of Department)

May 2005

Major Subject: Biomedical Engineering

ABSTRACT

Detection of Integrins Using Surface Enhanced Raman Spectroscopy. (May 2005)

Virgil Alexander Gant, B.S., Texas A&M University

Co-Chairs of Advisory Committee: Dr. Gerard L. Coté
Dr. Gerald A. Meininger

Integrins are transmembrane heterodimer protein receptors that mediate adherence to both the intracellular cytoskeleton and extracellular matrix. They play a major role in cellular adhesion and the breadth of their importance in biology is only recently being understood. The ability to detect concentrations of integrins on the cell surface, spatially resolve them, and study the dynamics of their behavior would be a significant advance in this field. Ultimately, the ability to detect dynamic changes of integrins on the surface of a cell maybe possible by developing a combined device such as an atomic force microscope (AFM) and surface enhanced Raman spectroscopy (SERS) system. However, the focus of this research is to first determine if integrins can be detected using SERS.

Surface enhanced Raman spectroscopy (SERS) is technique used to detect the presence of analytes at the nanomolar level or below, through detection of inelastically scattered light. This thesis discusses the detection of integrins employing SERS as the detection modality. Integrins have been detected, in solution, using two silver colloids as the enhancing surface. Two silver colloid preparation methods are compared by ease of formulation and degree of enhancement in this thesis. Citrate and hydroxylamine hydrochloride (HA-HCl) reduced silver colloids were prepared through wet chemistry,

compared using UV-Vis light spectroscopy, and tested for surface enhancement using adenine (a strong SERS active molecule), and two different integrins, $\alpha_V\beta_3$ and $\alpha_5\beta_1$. Results indicated that both colloids demonstrate SERS activity for varying concentrations of adenine as compared to standard non-enhanced Raman, however, only the citrate reduced colloid showed significant enhancement effect for the integrins.

To my family who has supported me in all of my endeavors.

ACKNOWLEDGMENTS

I am very thankful to my advisor Dr. Gerard Coté for his guidance throughout the course of my research and during my time in his lab group. I also want to thank Dr. Gerald Meininger and Dr. Lihong Wang for being a part of my committee.

I would especially like to thank Mustafa Chowdury who was instrumental in helping me understand the intricacies of surface enhanced Raman spectroscopy. I also am thankful to Angela Baldwin for assistance in collecting data and to Dr. Andreea Trache for introducing me to cellular research techniques and to Atomic Force Microscopy. I would like to thank the students in Dr. Coté's Optical Biosensing Laboratory for their numerous suggestions. Finally, I would like to thank everyone who has either directly or indirectly helped me complete my research and thesis.

TABLE OF CONTENTS

Page

Page

LIST OF FIGURES

FIGURE Page

LIST OF TABLES

TABLE Page

1. INTRODUCTION

1.1 PURPOSE OF RESEARCH

Integrins have been studied extensively since their discovery. Many approaches of research have been used to uncover more information about the various functions of integrins in cell development and remodeling [1]-[4]. Almost all of these methods of research rely on only one approach at a time to detect integrins. If two approaches were used simultaneously, it might be possible to answer questions that cannot be answered using only one approach [5]. The combination of two different systems to detect integrins and their reactions to various stimuli is a goal for collaboration between Texas A&M University Department of Biomedical Engineering Optical Biosensing Laboratory and Texas A&M University Health Science Center Department of Medical Physiology. The idea is to combine Atomic Force Microscopy (AFM) and Surface Enhanced Raman Spectroscopy (SERS) to detect the presence and accumulation of integrins during clustering when placed in close contact with extracellular matrix ligands. The ability to detect low concentrations of integrins on the cell surface, spatially resolve them and the study the dynamics of their behavior would be a significant advance in the field of biology.

This thesis follows the style of *IEEE Sensors*.

The proposed combined AFM-SERS system is illustrated in Figure 1. The AFM would be used with a functionalized tip that would serve two purposes. The AFM tip would be coated with a roughened layer of silver and would serve as the substrate surface necessary for SERS. The tip would also function as a platform to adhere RGD-sequenced ligands, such as fibronectin, through a polymerization process. SERS would be monitored from below the surface of the culture dish utilizing the inverted objective microscope to focus the laser onto the AFM tip. If the AFM system is used in force mode, the ligands polymerized to the AFM tip would induce integrin clustering and the SERS system would monitor the clustering based on the increase in concentration of integrins on the cell surface.

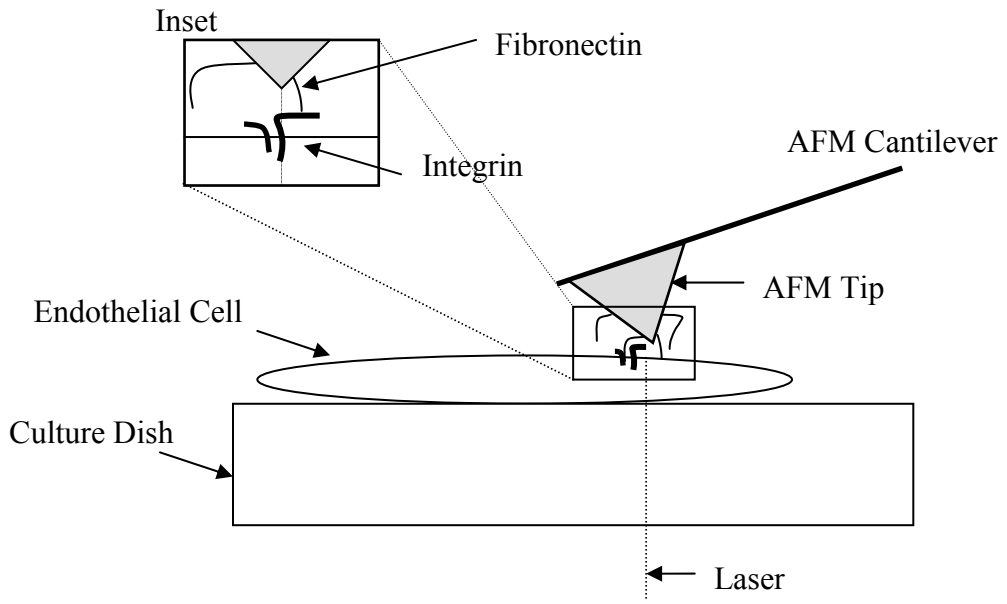

Figure 1. Proposed AFM-SERS setup for integrin detection.

Before this system can be realized, preliminary studies must be performed to assess whether the SERS system is at all sensitive to changes in integrin concentration and, if it is, can it be used to distinguish between different integrin types. Thus, the focus of this research is to ascertain this information using silver colloids in conjunction with two different integrins, $\alpha_V\beta_3$ and $\alpha_5\beta_1$. Before covering details the details of the work, a brief introduction of integrins, Raman spectroscopy, SERS, and AFM will be presented followed by an overview of the rest of the thesis.

1.2 INTEGRINS

Integrins are transmembrane heterodimer protein receptors that adhere to both the intracellular cytoskeleton and extracellular matrix. They can function as receptors for viruses and bacteria as well as play a critical role in the processes of thrombosis and cell development [6]. Integrins also act as signaling transduction pathways, passing signals from the extracellular matrix to the intracellular matrix and vice versa [7]. Because of their large involvement in cell processes, there is a large interest in further investigation into how integrins behave.

One of the main roles of integrins involves cell adhesion. This adhesion can be adhesion to other cells or to the molecules of the extracellular matrix. Integrins attach at one end to the extracellular matrix and at the other end to the intracellular molecules that form the cytoskeleton. The connection of the intracellular cytoskeleton, the extracellular matrix, and the integrin in between make up what is known as a focal adhesion. The two

parts of the heterodimer are two subunits, an α-subunit and a β-subunit, each of which is a long protein chain on the order of 200 kD in size [7]. There are at least twenty types of integrins that are currently known [8] and some integrins adhere to only one signaling ligand protein while other integrins adhere to various ligands [7].

Integrins signal bidirectionally across the cell membrane, that is both outside – in signaling and inside – out signaling can occur [9], [10]. Outside – in signaling is performed in integrins when the RGD (Arg-GLY-Asp) sequence of a ligand protein binds to the β-subunit of the integrin in the extracellular matrix (ECM) and subsequently causes the adhesion of the integrin to intracellular matrix proteins. This adhesion process is also known as the formation of a focal adhesion [9]. The proteins associated with the focal adhesion can also bind to each other creating a large network of proteins in a focal adhesion. Further signaling through this network of proteins can cause clustering of more integrins in the same region of the cell. Inside – out signaling occurs when cytoskelatal matrix proteins bind to β-subunit domains located within the cytoplasm and cause an increase in the head region binding affininty for other molecules [11]. The increase in binding affinity comes as a result of the head region, location of dimerization, "unfolding" and exposing itself further into the ECM [10]. This increased affinity will allow for an increase in the chance of ligand binding to the integrin and beginning outside – in signaling.

Integrins are also known to be involved in the proliferation of many diseases [7]. An example of an integrin facilitating in the spread of a disease is bacteria and microbes that will enter healthy cells by attachment to the integrins since the integrins act as

receptors to many molecules [12]-[14]. Cases of restenosis shortly after angioplasty have been caused by the increased activation of integrins on platelets [7]. Another example of how integrins could help spread disease in a patient is in cancer propagation. It has long been known that one of the main causes in the spread of cancer throughout a patient's body is by angiogenesis. When new blood vessels are formed endothelial cells as well smooth muscle cells are the cells that are most involved with the vessel formation. The integrin $\alpha_V\beta_3$ appears in endothelial cells and the smooth muscle cells (SMC) as the new blood vessels are forming. This integrin plays the major role in adhesion of the one endothelial cell or SMC to the next cell. If drugs or compounds are fabricated to block the $\alpha_V\beta_3$ adhesion, then angiogenesis could be curbed in the tumor and would subsequently cut off the development of future blood supply to the developing cancer [7]. This would be a major step in cancer research and the fight against cancer. Thus application of the knowledge of how integrins work would prove to be invaluable in the fight of many devastating diseases.

1.3 RAMAN SPECTROSCOPY

C.V. Raman and Krishnan observed in the 1920's that when monochromatic light passes through a liquid the wavelength of light scattered can change [15]. The scattered light is considered Raman scattered light and is lower in energy than the initial incident radiation. Rayleigh scattering is scatter in which there is no net change in the energy of the radiated molecule. Raman scattering is the result of absorption of energy by the

molecule. The energy is absorbed and dissipated in vibrational bands or modes of the molecule. Figure 2 shows a quantum mechanical energy diagram exhibiting the difference between Rayleigh scattering and Raman scattering.

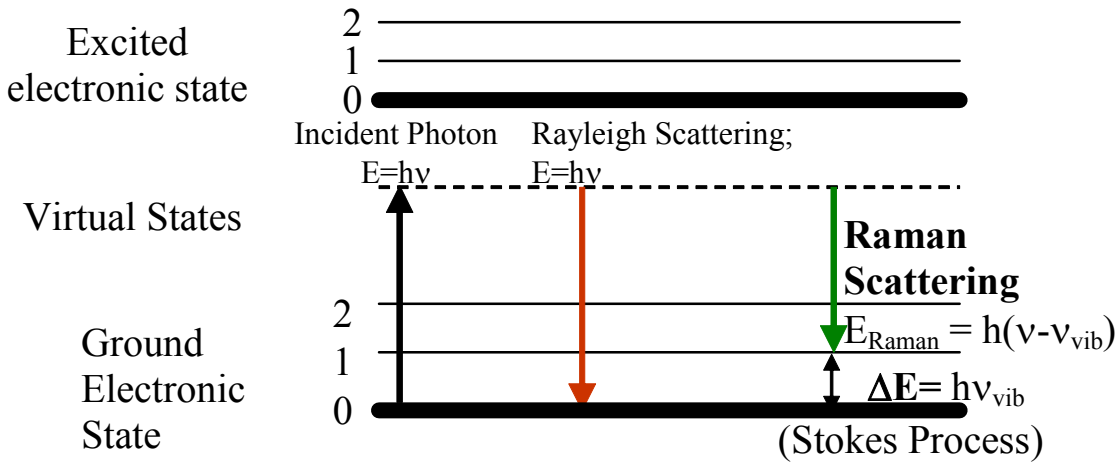

Figure 2. Quantum mechanical diagram of Rayleigh and Raman scattering. The vibrational states show the difference in emission photons associated with Rayleigh scattering and Raman scattering. Adapted from [16], [17]

The first arrow shows the energy contained in the incident photon, which strikes the molecule or analyte. The molecule is excited to a virtual excitation state and not a fully excited state. This occurs in both Rayleigh and Raman scattering. What happens after the excitation is the difference between the two forms of scattering. In Rayleigh scattering a photon is released with the same amount of energy as in the incident photon.

$$E_{total} = h\upsilon = h\frac{c}{\lambda}$$

where E_{total} is the total energy in the incident photon, h is Planck's constant, υ is the frequency, c is the speed of light, and λ is the wavelength in centimeters. This is also

called elastic scatter. Raman scattering is indicated in Figure 2 by the second emission arrow. The decrease in energy is smaller than in Rayleigh scattering. In Raman scattering, or inelastic scatter, the exiting photon leaves the molecule with less energy than the incident photon. The energy difference, as a result of the inelastic scatter, is lost to vibrations of the molecular bonds after the transfer of energy to the molecule:

$$\Delta E = h\upsilon_{vib}$$

where ΔE is the difference in energy and υ_{vib} is the vibrational frequency of the molecular bond that is vibrating. The exiting Raman scattered photon has less energy and is at a longer wavelength because the total energy of the incident photon must be conserved. Monitoring these inelastically scattered photons will give information about the vibrations occurring in the molecule.

$$E_{Raman} = h(\upsilon - \upsilon_{vib})$$

The molecular vibration observations make up a spectrum that is a deemed a Raman spectrum [16], [17].

Raman spectroscopy is complementary to another vibrational spectroscopy method, infrared spectroscopy. Infrared spectroscopy also gives bond vibration information but is based on the absorption of infrared light by the analyte. The peaks in each of the forms of spectroscopy describe similar vibrational bands in a spectrum and occur in comparable locations within the spectrum[16]. An enhanced method of Raman spectroscopy called surface enhanced Raman spectroscopy has the capability of detecting single molecules [18].

1.4 SERS

As mentioned, Raman Spectroscopy is an important method that has been used for researching the structure of biological macromolecules. However, this approach suffers from low sensitivity and the effects of background fluorescence [19]. Surface Enhanced Raman Spectroscopy (SERS) is a technique that generates a greatly enhanced Raman signal using lasers to excite vibrational transitions in molecules that are adsorbed onto certain metal surfaces [19]. The metal substrates are often in the form of colloids and electrodes, and are typically made of silver, gold, or copper [19]. SERS is advantageous because it has a sensitivity of 10^5-10^{12} times that of normal Raman Spectroscopy and has fluorescence quenching properties [19], [20]. SERS also displays surface selectivity because of enhancement mechanisms at the surface, making the bulk signal negligible [21].

The high sensitivity is primarily due to two cooperative mechanisms, an electromagnetic enhancement and a chemical enhancement [22]. The electromagnetic effects are mainly caused by localized surface plasmon resonance, or the excitation of oscillating surface electrons [23]. This enhancement is dominant and depends on the nanoscale surface roughness of the metal surface. The chemical mechanism contributes the other enhancement. It is believed to involve bonding interactions between the substrate and adsorbate, which cause the creation of new electronic states [24].

Though other methods have been used at metal surfaces, SERS has more adsorbate versatility, a broader wavenumber range, surface selectivity, and high

sensitivity [21], [18]. These advantages aide in the detection and structural analysis of naturally occurring low concentrations of biological molecules such as integrins.

1.5 ATOMIC FORCE MICROSCOPY

Atomic Force Microscopy (AFM) is a form of microscopy that relies on the tactile interaction with the specimen. Small forces on the order of piconewtons are applied to the sample using a tip on the end of a flexible cantilever and the reactionary forces are measured. The measured forces give quantitative information that can be resolved into the shape of the specimen to give a contour image or provide information regarding the surface stiffness of the sample.

The force is measured using the principles of spring loading. The cantilever will deflect a particular distance when a force is applied to end of the cantilever (the position of the tip). Using the following equation:

$$F = -kx$$

where k is the force constant inherent to the cantilever and x is the distance the cantilever deflects a force value can be obtained. The force constant of the cantilever is determined at the time of manufacture.

The detection of the deflection of the cantilever or the force applied to the sample is determined using a laser and a segmented photodiode. The top of the cantilever is gold coated and reflective. A low power He-Ne laser is focused and reflected off the gold top surface of the cantilever. The reflected laser is then detected by a segmented

photodiode. As the cantilever is deflected, the laser will be directed onto a different location on the photodiode. This signal is recorded and subsequently used in a feed-back control loop to continually reset the height of the tip so that the force applied to the sample remains relatively constant (Fig 3).

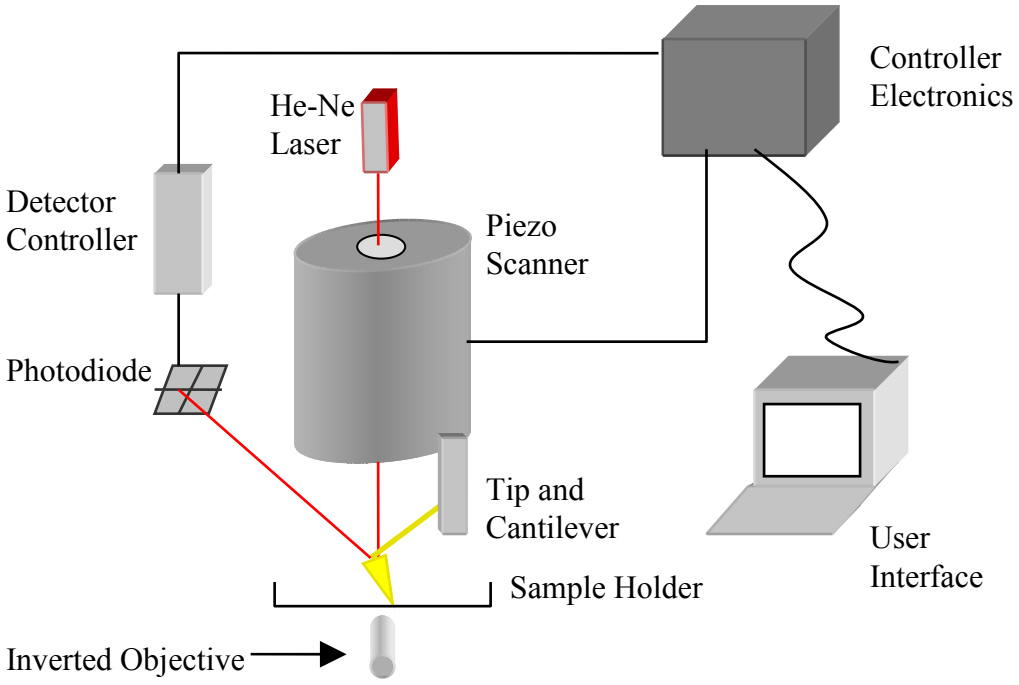

Figure 3. Atomic Force Microscope (AFM) setup.

The piezo scanner is the piece of the AFM that controls fine movement in three dimensions. The X and Y dimensions is capable of up to 100 µm movement whereas the Z-direction is limited to around 10 µm. The movement of the piezo is controlled continuously during a scan by the electronics controller by a feedback loop which monitors the position of the cantilever.

There are two main modes of operation when using an AFM, imaging mode and force mode. Imaging mode will obtain images of the sample by performing a rasterized scan over the surface of the sample. Height information for all points in the raster scan will form a contour image of the surface.

In force mode, the tip is repeatedly moved only in the vertical Z-dimension. The tip is moved into contact with the surface and the cantilever is flexed and deformed based on the inherent spring constant of the cantilever. The tip and cantilever is then removed from the surface of the sample. Adhesion can be observed when a negative force is seen by the cantilever. When adhesion occurs, the cantilever deforms in the opposite direction from the situation when the cantilever applies force to the sample surface in the first half of a force measurement and is moving toward the sample.

The AFM tip can be functionalized by adhering extracellular matrix proteins using a polymerizeration process [1]. Functionalizing the AFM tip allows for the measurement of binding forces between matrix proteins and the integrins that occur in a focal adhesion.

1.6 OVERVIEW

Given this brief introduction it is reiterated here that the focus of this report is the collection of SERS data and its subsequent analysis to detect integrins isolated in solution. The first part of Section II discusses the preparation of the aqueous silver colloids that provide the metal surface that is necessary to obtain surface enhanced Raman spectra. Following the preparation of the colloids, testing the specific sensitivity of the silver colloids is vital to the experimental process before actually testing the SERS response of integrins due to cost constraints. The colloid tests and experiments are covered in the second half of Section II. Adenine is a highly SERS responsive molecule and it is used to test the ability of the silver colloids to provide ample surface enhancement. A set of SERS data was collected in order to establish a proper and consistent protocol when collecting the data. SERS spectra of various concentrations of adenine were collected to show that it was possible to detect changes in analyte concentrations using the newly formed colloids. Once the colloids were shown to be capable of producing SERS concentration trends in adenine, SERS spectra of varying concentrations of $\alpha_V\beta_3$ and $\alpha_5\beta_1$ were obtained. The results are discussed in detail in Section III. Section IV briefly discusses the conclusions formed in this thesis and the future work that needs to be done to further the findings in this thesis.

2. SILVER COLLOIDS

2.1 SILVER COLLOID PREPARATION

Colloids are a system in which particles of colloidal size (1 nm to 1 μm) of any nature (e.g. solid, liquid or gas) are dispersed in a continuous phase of a different composition (or state) [25]. Silver particles on the order of 10 nm [26] were formed in water making a silver colloid. Two separate silver colloids using different preparation methods were created so that a comparison could be made between the two methods. The first preparation method was a citrate reduced colloid. This is a well established preparation method but can be difficult at times to prepare due to the non-standardized boiling time [26]. The second prepartion method is a newer protocol that requires no prolonged reaction time and can be carried out at room temperature [27]. This protocol is a hydroxylamine–hydrochloride reduced silver colloid. It is clear that the hydroxylamine–hydroxylamine reduced colloid is easier to prepare. However, a comparison of the ability of each of the colloids to provide surface enhancement for the analyte of interest, namely the integrins, provide evidence for which colloid is better.

2.1.1 Citrate Reduced Colloids

The citrate reduced silver colloids were prepared in accordance with the protocol established by Lee and Meisel [26]. Silver nitrate ($AgNO_3$), 45 mg, obtained from Alfa Aesar, Wade Hill, MA was dissolved in deionized water (H_20), 250 mg, to form a 1.05 mM solution. The solution was then heated to a boil. A 1% solution of sodium citrate

($C_6H_5Na_3O_7$) also obtained from Alfa Aesar, was then prepared with 50 mg sodium citrate diluted in 5 mL of water. The sodium citrate solution was also brought to a boil and then added to the boiling silver nitrate solution. The entire solution was stirred continuously and allowed to boil for one hour and then quickly cooled in a water bath in order to stop all reaction.

2.1.2 Hydroxylamine-Hydrochloride Reduced Colloids

A second silver colloid was prepared according the procedure described by Leopold and Lendl [27]. The hydroxylamine hydrochloride ($NH_2OH{\cdot}HCl$) reduced colloid was prepared by adding 10 mL of silver nitrate (1×10^{-2} M) to a 90 mL hydroxylamine hydrochloride (1.67×10^{-3} M) and sodium hydroxide (NaOH) (3.33×10^{-3} M) solution. This mixture was formed at room temperature under rapid stirring conditions. The final concentrations in the mixture of silver nitrate and hydroxylamine hydrochloride / sodium hydroxide was 1×10^{-3} M and 1.5×10^{-3} M / 3×10^{-3} M, respectively.

Another way of forming the hydroxylamine hydrochloride reduced silver colloid was to add the hydroxylamine hydrochloride / sodium hydroxide solution to the silver nitrate solution in order to achieve the aforementioned final concentrations. This secondary colloidal preparation was done by adding 10 mL of a higher concentrated hydroxylamine hydrochloride / sodium hydroxide (1.5×10^{-2} M / 3×10^{-2} M) solution to a 90 mL lower concentrated silver nitrate solution (1.11×10^{-3} M).

2.2 COLLOID ANALYSIS

Experiments were conducted to determine the sensitivity of the colloids to provide a SERS enhancement on analytes known to produce a strong SERS signal. The capacity for SERS enhancement by the prepared colloids was carried out by performing Ultraviolet-Visible (UV-Vis) absorption tests and SERS experiments on adenine analytes that has been known to give off strong SERS spectra [28].

2.2.1 UV-Vis Absorption Experiments

Once the colloids were prepared, a UV-Vis absorption spectrum was obtained in order to determine at what wavelength range absorption occurred. The peak absorption occurs at about 418 nm for the hydroxylamine hydrochloride reduced colloids and about 430 nm for the citrate reduced colloids. The quality of the colloid could also be determined by this peak absorption at either 418 nm or 430 nm. The Full Width / Half Maximum (FWHM) of the peak gives insite into the uniformity of the colloid [26],[27],[29]. The UV-Vis absorption data was collected using a Beckman DU® 640 Spectrophotometer. The colloids were were diluted 1:5, colloid to water, so that the spectrophotometer did not saturate. Once the colloids had been characterized by using UV-Vis absorption spectra, the colloids were observed to determine if they would remain in solution and not become silver slurries that has been known to occur if the colloid falls out of solution.

The absorption spectra of the 1:5 diluted colloids is depicted in Figure 4. Figure 4 also shows some examples of the problems faced when preparing a good set of citrate

reduced colloids as well as hydroxylamine hydrochloride reduced colloids. The spectra labeled “A”, “B”, and “C” are extinction spectra of three batches of colloid formed using the citrate reduced method. The spectrum labeled “A” had the largest extinction and was used in the subsequent SERS tests for this reason. The extinction is not a true account of absorption of energy because scatter is also included in extinction but is used as an estimation of the true absorption. The difference in the maximum extinction of “A”, “B”, and “C” illustrates the variability that can exist when boiling the citrate reduced colloids.

The spectra labeled “D” and “E” are extinction spectra of two batches of colloids formed using the hydroxylamine hydrochloride reduction method. The extinction spectrum labeled “D” was the colloid used during the SERS experiments. The spectrum labeled “E” was prepared using the secondary method of hydroxylamine hydrochloride reduced colloid preparation as previously described in section 2.1. The colloid labeled “D” was chosen because the peak extinction occurred at a wavelength close to the “ideal” 418 nm wavelength for this colloid.

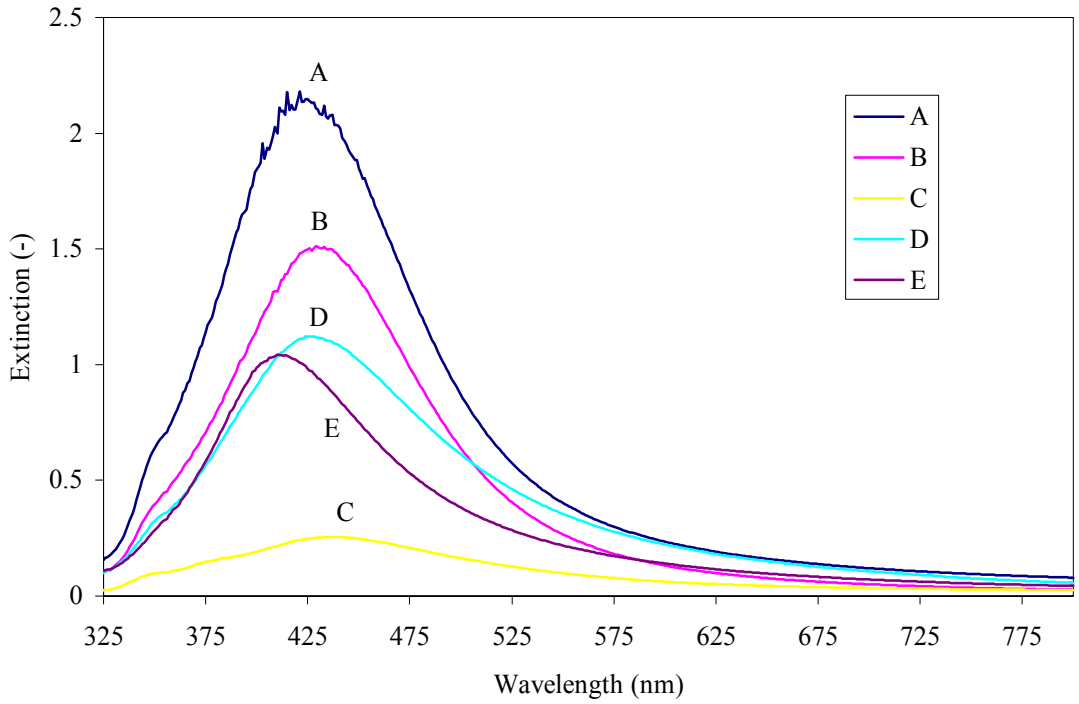

Figure 4. Extinction of colloid batches. Batches A-C were formed using the citrate reduced colloid preparation method. Batches D and E were formed using the hydroxylamine hydrochloride reduced preparation method.

2.2.2 SERS Analysis of Colloids

The colloids chosen from the UV-Vis absorption tests were then subjected to SERS testing using analytes that are known to provide strong SERS signatures as well as allowing the colloid to adsorb well to the analyte. The analytes used were congo red and adenine. All SERS experiments were carried out using the same protocol. The Raman spectrometer setup seen in Figure 5 was used in all Raman and SERS experiments. A 50 µL cylindrical sample well was used in all Raman experiments.

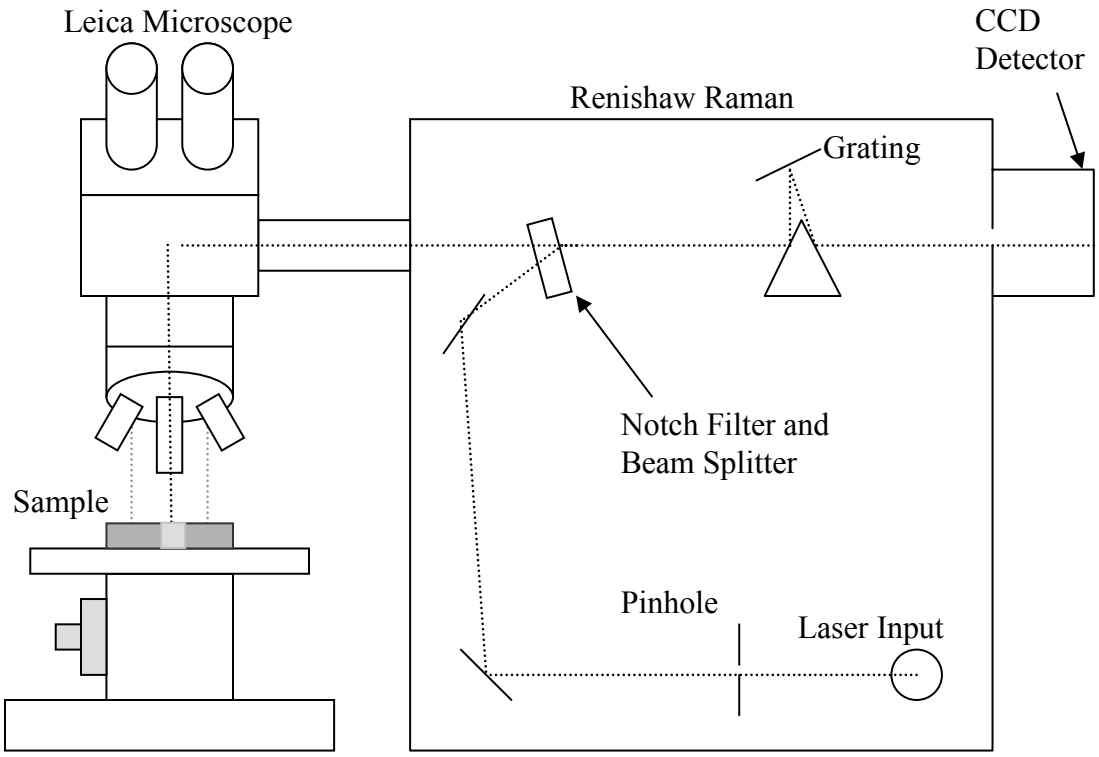

Figure 5. Raman spectrometer and microscope. The dotted line represents the path of the laser through the Raman spectrometer.

2.3 RAMAN SPECTROMETER SETUP

All SERS spectra were collected using a Renishaw System 1000 Raman Spectrometer coupled to a Leica DMLM microscope (Fig 5). The laser used in the system setup was a 514.5 nm Ar^+ laser (Spectra Physics Model 263C) operating at a power of 45 mW. After a coupling efficiency of 10 %, 4.5 mW was delivered to the

sample. The laser enters the Raman spectrometer through a hole in the rear of the spectrometer, labeled “Laser Input”. The laser is then reflected off of a mirror through a pinhole setup that removes laser speckle and focuses the beam. Subsequently the laser beam is directed to a beam splitter. The beam splitter allows incident light at one angle to pass through while at other angles the light is reflected. The laser is reflected and directed by the beam splitter into the microscope to excite the sample using a 5x objective. The excited Raman signal is then returned at 180° to the incident light back up into the microscope. The Raman signal then re-enters the Raman spectrometer and then passes through the beam splitter and an angle that allows the light to pass. Next, the light passes through a holographic notch filter that cuts out the narrow band of laser emission. The remaining signal, after passing through the notch filter, is the Raman scattered signal and is then spread into a spectrum when it is directed off a very high groove count grating. The spectrum is finally captured on a charge-coupled device (CCD) detector. A computer running Renishaw WiRE^{TM} software (version 1.2) controls the Raman spectrometer and also is used to perform a baseline correction routine.

In order to setup the Raman spectrometer for experimental use a focusing procedure had to be carried out at the start of all experiments. Fifty μL of Dimethyl sulfoxide (DMSO) was placed in the well and set on the sample stage. DMSO is used for focusing purposes due to its strong Raman signal. DMSO has an index of refraction of 1.4780 whereas water has index of refraction of 1.3333. Water is the majority of the makeup of all the SERS samples and the index of refraction mismatch could cause reason for concern. The incident light on the sample is always at 90° to the sample

surface and therefore not a problem. Carbon tetrachloride (CCl_4) is another molecule that can be used for focusing but is toxic and a carcinogen. Two and a half second (2.5 sec) integration time continous Raman scans of DMSO were captured to serve as a measure when focusing the microscope. When the strongest Raman signal was present the microscope was focused and the Raman experiments could begin (Figure 6).

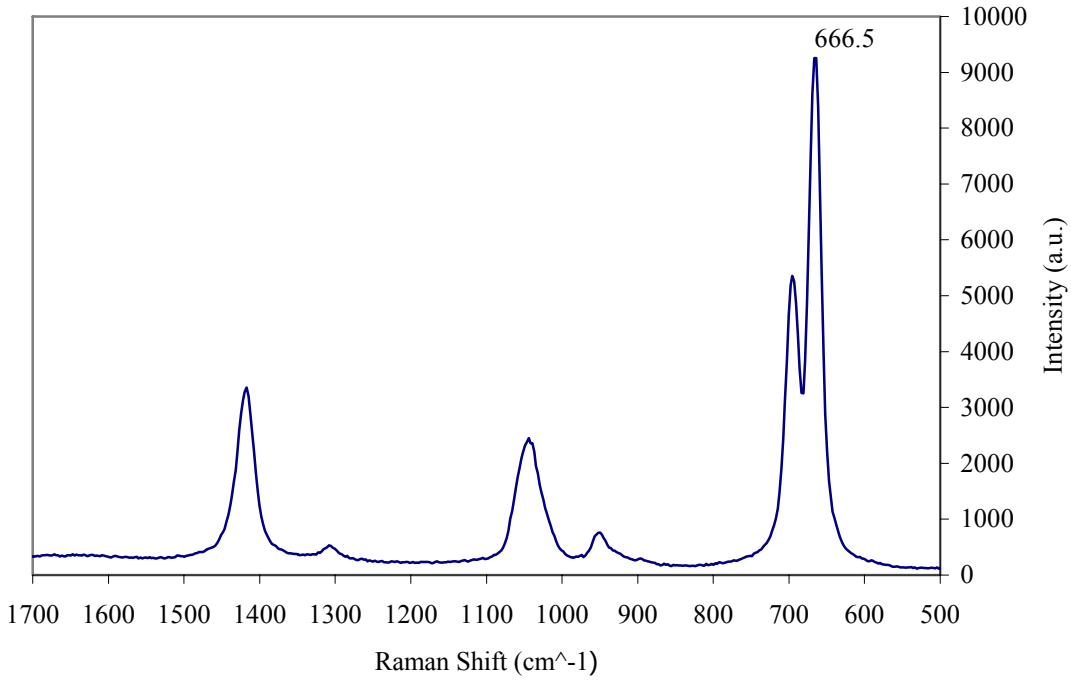

Figure 6. Raman spectrum of dimethyl sulfoxide (DMSO). The sample was scanned for 2.5 sec. The microscope is in focus when the Raman signal of DMSO is at its maximum (666.5 cm^{-1}).

The SERS samples were prepared in solution. The SERS samples of adenine were prepared in the following steps. Five (5) µL of 1.0 M concentration NaCl was added to 50 µL of silver (Ag) colloid, either the citrate reduced colloid or the hydroxylamine hydrochloride reduced colloid in order to activate the colloid, to begin the aggregation process. After uniform mixing of the colloid and salt solution 5 µL of

the adenine sample solution was added to the aggregating colloidal solution. Fifty (50) μL of the final complete mixture were then placed in the 50 μL sample well and was then place on the microscope stage to be analyzed.

The SERS spectrum of adenine exhibits two strong peaks located at 730 cm^{-1} and at 1325 cm^{-1} (Figure 7). In addition to the two strong peaks that lie at the same Raman shift, the colloids both have other minor peaks indicating similar Raman shifts. The results show that both colloids work well to enhance the Raman spectrum of adenine. However, the presence of more well defined peaks when using the hydroxylamine-hydrochloride reduced colloid indicates that adenine adsorbs better to the colloid yielding a cleaner signal.

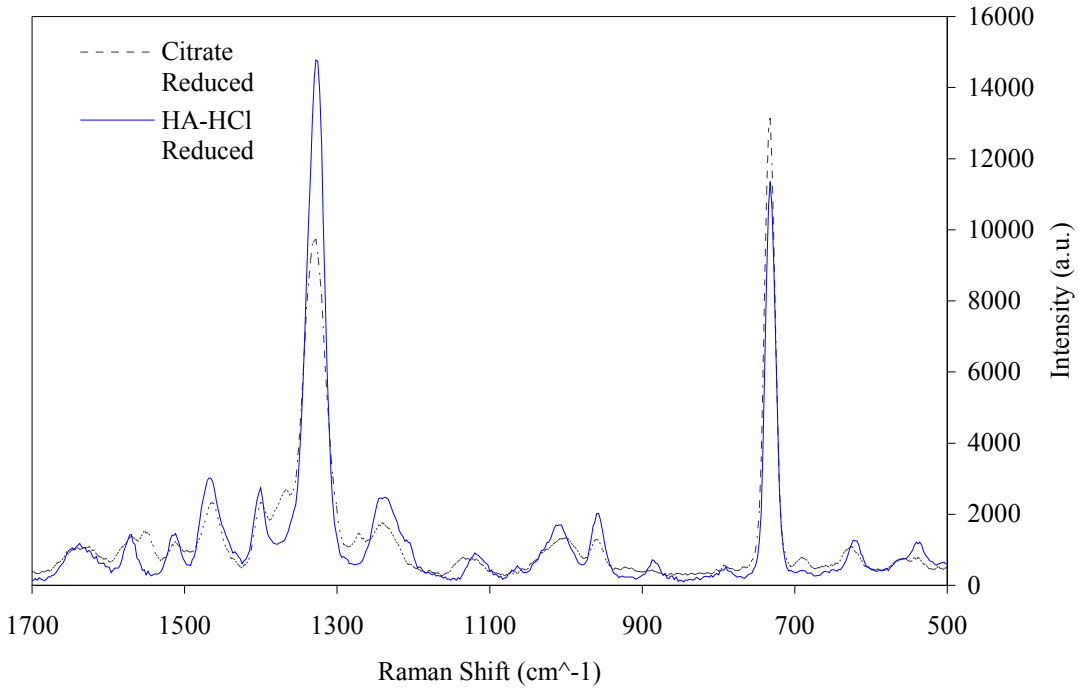

Figure 7. SERS spectra of adenine. The 44.0 μM adenine was enhanced with the citrate reduced colloid and the hydroxylamine colloid. The two large, sharp peaks at 730 cm^{-1} and at 1325 cm^{-1} are used to perform concentration studies.

The focus of the SERS concentration studies revolved around the two sharp peaks at 730 cm^{-1} and at 1325 cm^{-1}. These two peaks were used as indicators of the various concentrations tested. Both of the colloids used showed that a concentration study was possible and that detection down to the nM concentrations was achieved. The linear region of detection is along a sigmodal signal response falls between 4 and 40 µM (Figures 8 and 9). Because the capability of the colloids to perform a concentration study using SERS was shown, it was feasible to obtain SERS spectra of integrins.

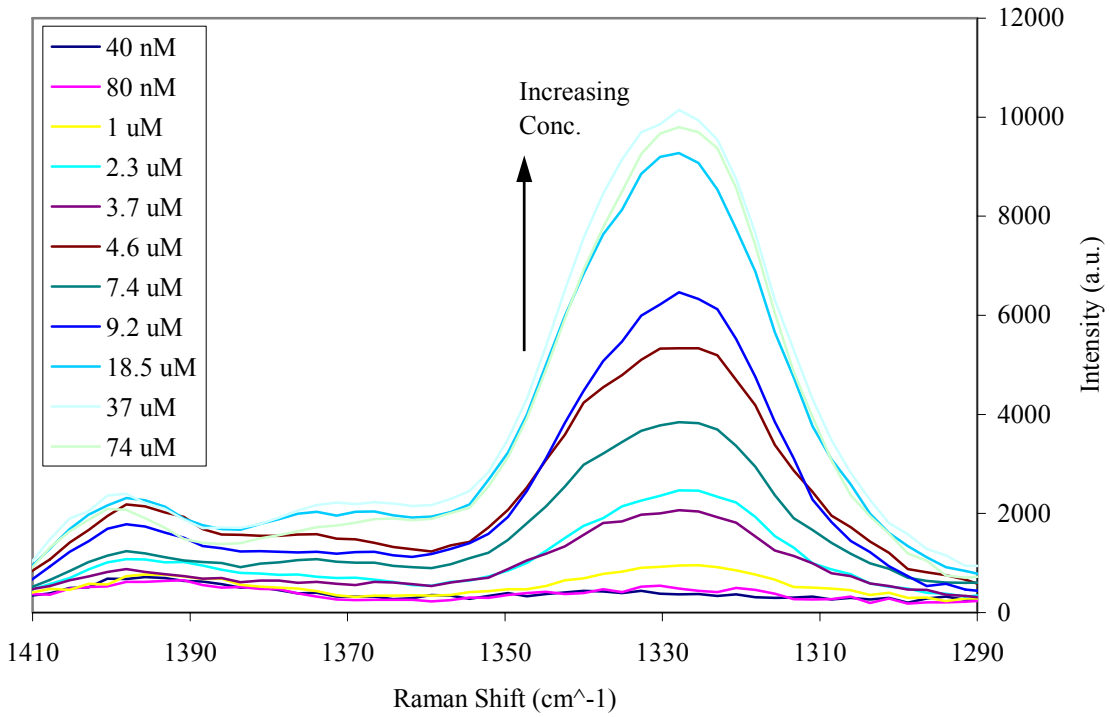

Figure 8. Adenine concentration response with citrate reduced colloid. The peak at 1325 cm^{-1} was monitored.

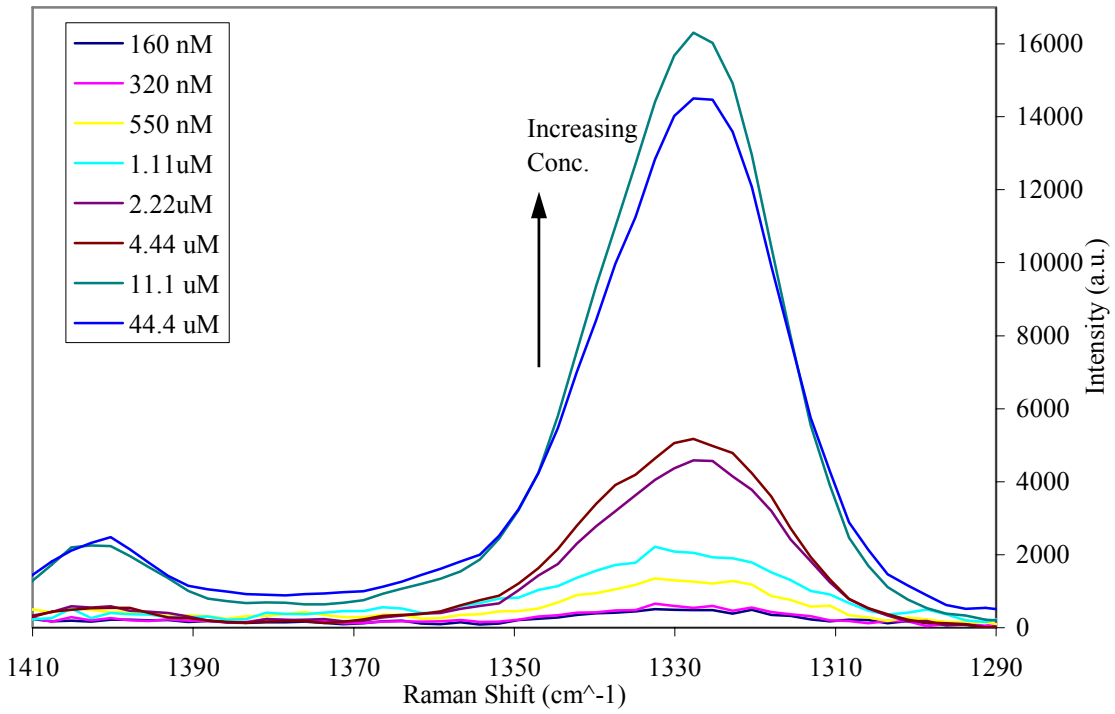

Figure 9. Adenine concentration response with HA-HCl reduced colloid. The peak at 1325 cm^{-1} was monitored.

3. INTEGRIN STUDIES

Two different types of integrins were analyzed in this study, $\alpha_V\beta_3$ and $\alpha_5\beta_1$. These are two integrins of interest due to their known contribution to roles within cardiovasular endothelial cells and their implications in angiogenisis within tumors [4]. Integrins $\alpha_V\beta_3$ and $\alpha_5\beta_1$ regulate the contractility of arterioles: $\alpha_V\beta_3$ induces a vasodilator response in the vasculature while $\alpha_5\beta_1$ induces a vasoconstriction response [4], [30], [31].

The two integrins of interest were analyzed using two separate SERS experiments. The first set of experiments was performed to analyze the SERS spectra given off by the integrins and to determine if a unique SERS spectrum is given by each of the integrins. In the second set of integrin experiments a concentration study was performed. The feasibility of creating a SERS concentration response for each of the integrins was explored. A successful concentration response illustrating an increase in SERS signal corresponds to an increase in the concentration of integrin in solution is imperative for future studies using both AFM and SERS to analyze the formation of focal adhesion points of integrins within cultured cells. A measure of increased integrin concentration would signal the formation of a focal adhesions and integrin clustering.

3.1 SPECTRAL ANALYSIS

3.1.1 Experimental Setup

Studies were initially carried out to obtain SERS spectra of pure integrins and subsequently analyze the SERS signatures given off by the integrins. The Raman spectrometer setup employed for this experiment is the same as previously described in section 2.3. Pure human integrins $\alpha_V\beta_3$ and $\alpha_5\beta_1$ were purchased from Chemicon International, Temecula, CA (Cat. # CC1020 and CC1026, respectively). The $\alpha_V\beta_3$ integrin stock concentration was 350 μg/mL (1.456 μM) and came as a 25 μg stock solution giving a total sample volume of 70 μL in a β-D-Glucopyranoside based buffer. β-D-Glucopyranoside keeps the conformational structure of the protein intact [32]. The $\alpha_5\beta_1$ integrin stock concentration was 418 μg/mL (1.58 μM) and came as a 25 μg stock solution giving a total sample volume of 60 μL. The $\alpha_5\beta_1$ integrin also came in the β-D-Glucopyranoside buffer. The molecular weights of the integrin subunits are as follows: α_V subunit is 150 kDa, β_3 subunit is 90 kDa, α_5 subunit is 155 kDa, β_1 subunit is 110 kDa giving the total molecular weight of the integrins is 240 kDa for $\alpha_V\beta_3$ and 265 kDa for $\alpha_5\beta_1$.

The SERS samples were prepared in solution. The SERS samples of integrin $\alpha_V\beta_3$ were prepared in the following steps. Five (5) μL of 1.0 M concentration NaCl was added to 50 μL of silver (Ag) colloid, either the citrate reduced colloid or the hydroxylamine-hydrochloride reduced colloid in order to activate the colloid and begin the aggregation process. After uniform mixing of the colloid and salt solution 5 μL of

the stock $\alpha_V\beta_3$ solution was added to the aggregating colloidal solution. This yielded a final $\alpha_V\beta_3$ integrin concentration of 122 nM within the aqueous colloid solution. Fifty (50) μL of the final complete mixture were then placed in the 50 μL sample well.

For the formation of the $\alpha_5\beta_1$ integrin SERS samples, 6 μL of 1.0 M NaCl was added to 60 μL the Ag colloid to begin the aggregation process. After thorough mixing of the colloidal mixture, 6 μL of the stock $\alpha_5\beta_1$ integrin was added. This yielded a final concentration of 131 nM of $\alpha_5\beta_1$ within the aqueous colloid solution.

In order to conserve integrin, the protocol for the two different integrins comes from sample conservation. Initially the $\alpha_5\beta_1$ integrin sample was formed using the 60:6:6 (60 μL colloid : 6 μL NaCl : 6 μL analyte) protocol to allow for the extraction of the necessary 50 μL to fill up the Raman sample chamber. A total of 72 μL would allow for a full 50 μL sample to be extracted from the mixing cuvette without any air pockets entering the pipette. In order to limit the integrin sample the protocol was changed to use only 5 μL of stock integrin solution at a time by employing a 50:5:5 SERS sample mixture. This was carried out with the $\alpha_V\beta_3$ integrin whereas the protocol for the $\alpha_5\beta_1$ integrin remained as 60:6:6.

As soon as the sample solution was prepared, the 50 μL sample solution was loaded into the Raman sample chamber. The SERS spectra were then collected using an integration time of 150 seconds for each scan and consecutive scans were taken, varying from four to eight, depending on the sample. The Raman spectrometer was centered at 1200 cm^{-1} wavenumbers for all spectra. The results of the SERS detection of the two integrins were then analyzed.

The SERS spectra recorded for integrins were all treated in the same manner. First, all of the integrin spectra was captured by the Raman spectrometer and recorded by the computer. At the end of the collection of data pertaining to the integrins, SERS spectra were recorded of the buffer solution to serve as a background and subsequently subtracted from the raw data. Following the background subtraction, a four-point baseline correction is performed using Renishaw WiRE^{TM} software (version 1.2). A raw integrin spectrum, a background spectrum, and a spectrum of the same raw data analyzed is displayed in Figure 10.

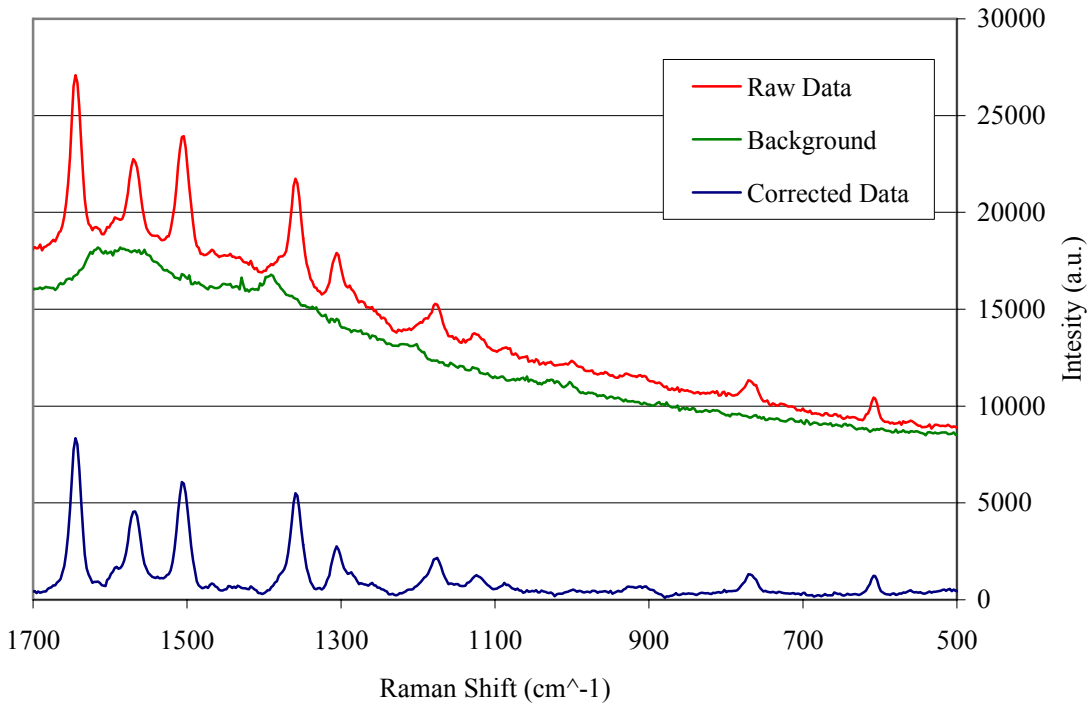

Figure 10. Integrin spectrum data analysis. The top spectra (highest intensity) is a raw SERS spectrum of $\alpha_5\beta_1$ top spectrum. The middle spectrum is a background SERS spectrum of the buffer solution. The bottom spectrum is a background subtracted and baseline corrected spectra of the original raw spectrum.

3.1.2 Results and Discussion

The SERS spectral peaks are a result of the structure and shape of the large heterodimer proteins and how well the protein adsorbs onto the surface of the silver colloids [19]. SERS spectra were obtained of both $\alpha_V\beta_3$ and $\alpha_5\beta_1$ using the citrate reduced colloid (Figs 11 and 12).

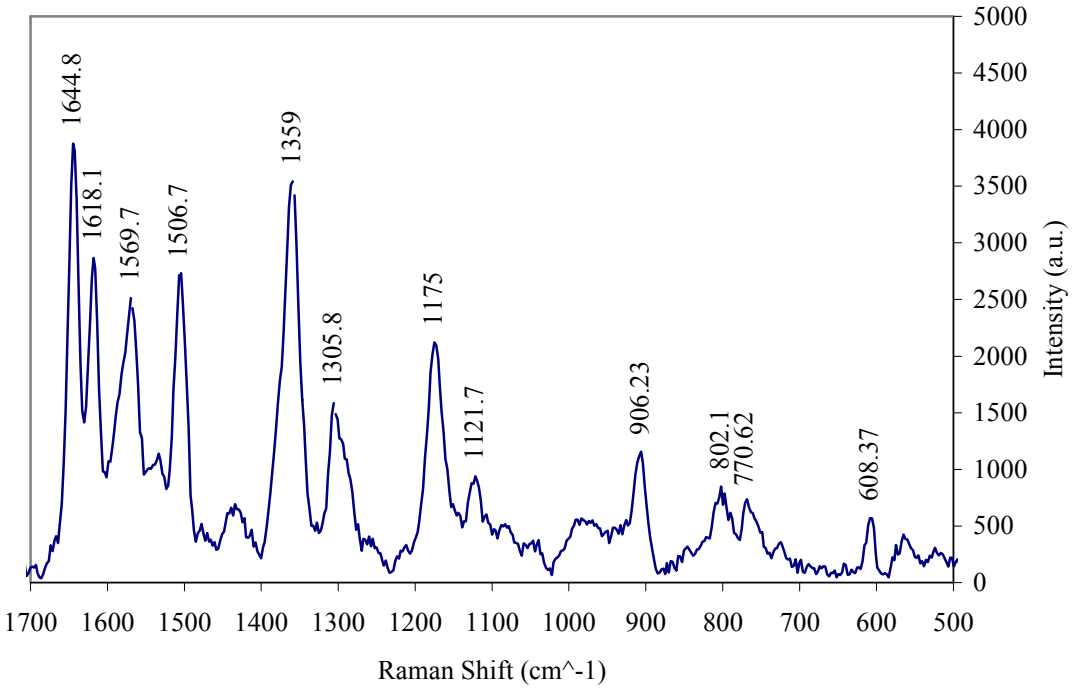

Figure 11. SERS spectrum of $\alpha_V\beta_3$ using citrate reduced colloid. The peaks and bands associated with the protein structure are labeled.

The two integrins have many of the same peaks in common with one another. A summary of all peak assignments associated with both of the integrins $\alpha_V\beta_3$ and $\alpha_5\beta_1$ is displayed in Table 1. The peak located at 1644.8 cm^{-1} is from the amide I band and is indictative of an α-helix structure [19], [20], [33]. The amide I band comes from stretch

vibration of carbonyl double bond in the peptide backbone. The peak located at 1305.8 cm^{-1} is from the amide III band and is further indication of the presence of α-helix [19], [20], [33]. In addition to the 1305.8 cm^{-1} peak there are shoulder peaks at 1288 cm^{-1} and 1259 cm^{-1} which also reside in the amide III band. The specific peak at 1305.8 cm^{-1} further indicates the presence of an α-helix [19]. An α-helix is a large portion of the structure of both dimers α_V and α_5 [11].

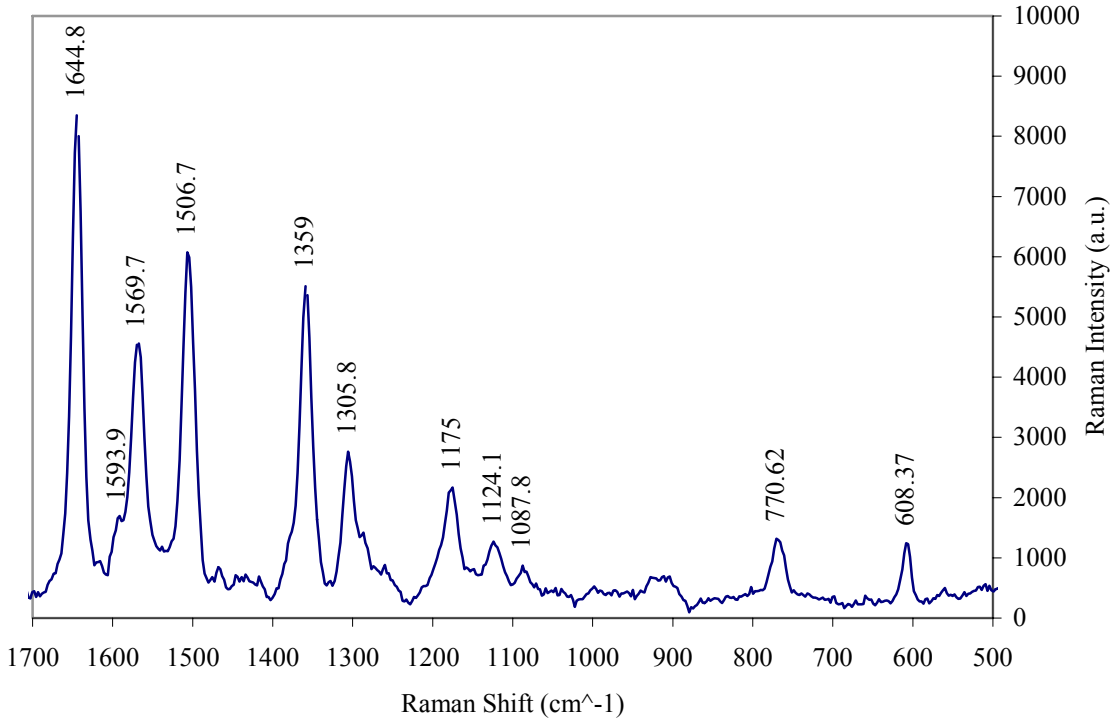

Figure 12. SERS spectrum of $\alpha_5\beta_1$ using citrate reduced colloid. The peaks and bands associated with the protein structure are labelled.

The amino acids with aromatic rings phenylalanine, tryptophan, and tyrosine give off strong SERS signals [19], [20], [33], [34]. Another amino acid that also gives off SERS signal is histidine. Histidine does not have aromaticity, but its two alternating double bonds in the imidazole ring provide vibration in a similar way to the aromatic

amino acids to give a SERS signal. Peaks that are seen in SERS spectra of both integrins from aromatic ring vibrations are prevalent at 1569.7 cm^{-1}, 1506.7 cm^{-1}, 1359 cm^{-1}, 1175 cm^{-1}, 770.62 cm^{-1}, and 608.37 cm^{-1}. More specifically, the phenylalanine and tyrosine bands are the peaks at 1506.7 cm^{-1}, 1175 cm^{-1}, 770.62 cm^{-1}, and 608.37 cm^{-1}. The tryptophan and histidine bands are the peaks found at 1569.7 cm^{-1}, 1359 cm^{-1}, and 770.62 cm^{-1}.

Although the spectra of the two integrins exhibit many of the same peaks and bands, the spectrum of integrin $\alpha_V\beta_3$ shows more peaks. In addition to the peaks previously mentioned, peaks occur at 1618.1 cm^{-1} and 906.23 cm^{-1}. The 1618.1 cm^{-1} peak is indicative of either phenylalanine or tyrosine [19]. The 906.23 cm^{-1} is indicative of the (Cα-C-N) peptide bond in stretch vibration [33]. The integrin $\alpha_5\beta_1$ has small peaks at 1124.1 cm^{-1} and 1087.8 cm^{-1} that as a pair indicate vibration in the peptide bond (C-N) [33].

Table 1. Assignments of SERS spectral peaks for $\alpha_V\beta_3$ and $\alpha_5\beta_1$

Frequency (cm^{-1})		Assignment
$\alpha_V\beta_3$	$\alpha_5\beta_1$	
1645	1645	Amide I Band & α-helix
1618	-	Phenylalanine or Tyrosine Residues
1569	1569	Tryptophan or Histidine Residues
1506	1506	Phenylalanine, Tyrosine, or Histidine Residues
1359	1359	Tryptophan Residue
1305	1305	Amide III Band & α-helix
1175	1175	Phenylalanine or Tyrosine Residues
-	1124	(C-N) peptide bond stretch vibration
-	1087	(C-N) peptide bond stretch vibration
906	-	(C_α-C-N) peptide bond stretch vibration
770	770	Tryptophan or Histidine Residues
608	608	Phenylalanine Residue

SERS spectra were obtained of integrin $\alpha_5\beta_1$ using the hydroxylamine hydrochloride reduced colloid but did not show any of the clear, sharp peaks that were seen with the citrate reduced colloid (Figure 13).The same trial was tried an additional three times but the outcome was the same in each subsequent trial.

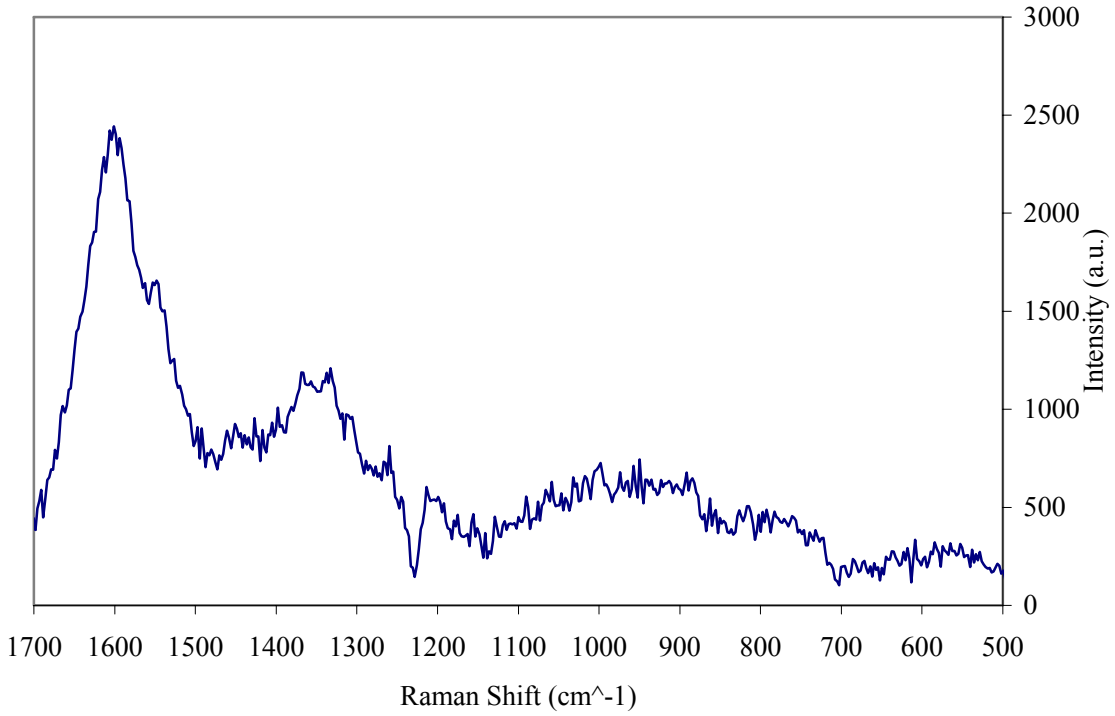

Figure 13. SERS spectrum of $\alpha_5\beta_1$ HA-HCl reduced colloid. Only the large broad band at 1606 cm^{-1} may indicate the Amide I band.

There is a large broad peak centered around 1600 cm^{-1} that may be the amide I band. There also some other areas in the the spectrum that could be considered peaks which reside in regions in the spectrum associated with protein but the signal to noise ratio is too low to make specific assignments.

The poor SERS response when using the hydroxylamine hydrochloride reduced colloid is possibly a result of poor adsorption of the integrin onto the colloid. Poor adsorption would explain why the usually strong and sharp Amide I band is present but is not sharp as was shown in the SERS spectra citrate reduced colloid spectra . This could indicate unfavorable conditions for adsorption such as the pH of the colloidal solution or surface charges of the silver particles were not conducive for providing SERS [33]. The pH of both colloids before and after NaCl aggregation was tested to verify this claim. The pH of the citrate reduced colloidal solution was found to be 7.59 before NaCl aggregation and 7.54 after aggregation. The pH of the hydroxylamine hydrochloride reduced colloid was 6.15 before aggregation and 5.95 after aggregation. The large difference in pH between the colloids could definitely affect the integrin adsorption onto the silver particles. Beyond affecting only the adsorption, the acidic environment of the hydroxylamine hydrochloride colloid could have denatured the structure of the integrin protein. The pH of the citrate reduced colloid falling in the biological range makes the denaturation case plausible. The constancy of the four trials adds further evidence for the claims of poor adsorption and denaturation.

In addition to simply analyzing what peaks are present in the SERS spectra, a time progression of the adsorbance of the integrin onto the silver surface was also conducted. As the consecutive scans were collected it was noticed that only in the $\alpha_V\beta_3$ the appearance of the peak at 1618.1 cm^{-1} seemed to be increasing at a greater rate than the rise of other peaks as the integrin adsorbed to the silver colloid. If the peak was increasing at a faster rate, this could indicate a kinetic interaction taking place. Further investigation of the legitamacy of this observation was required, and so the peak heights were anaylzed in reference to a spot at the base of the peak from the amide I band (1644.8 cm^{-1}). The base point where it was deemed that no other SERS peaks could have superimposed was at 1660 cm^{-1}. The difference between the intensity height of the peak (1644.8 cm^{-1} and 1618.1 cm^{-1}) and the neutral base point at 1660 cm^{-1} were recorded and plotted (Fig. 14). The ratio of the peak intensities shows that after an initial increase from the first scan to the second scan, the relative intensity between the two peaks does not significantly change (Fig. 15), therefore, a complex kinetic interaction did not occur. It was found to be only superposition of the tails of surrounding peaks.

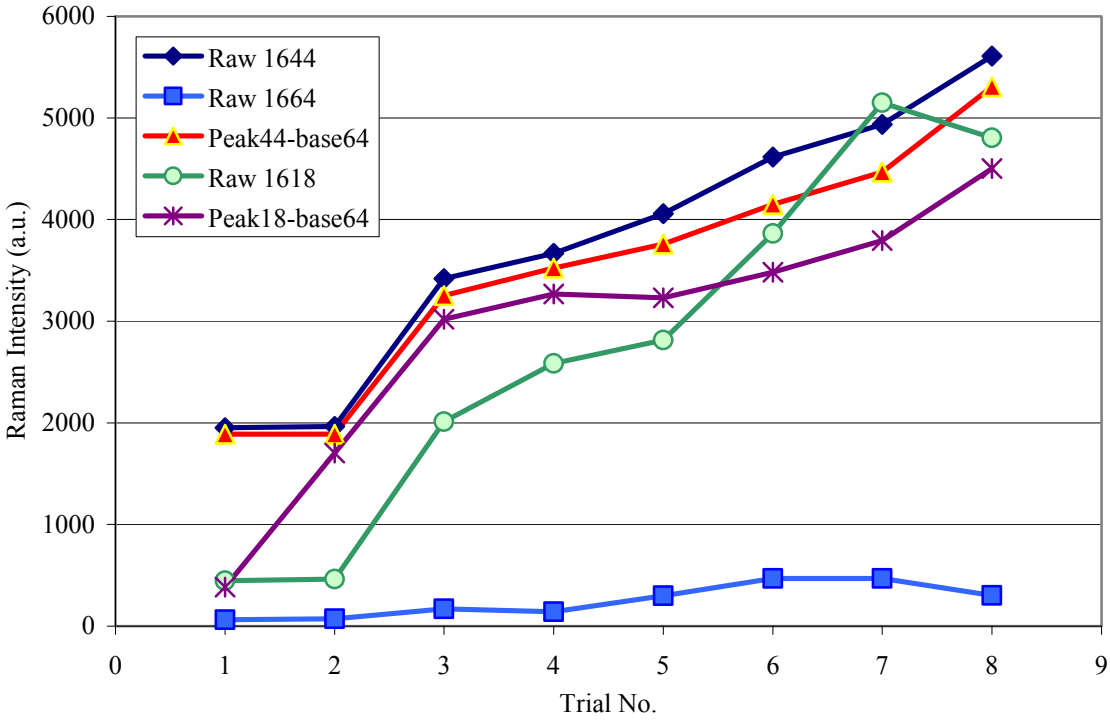

Figure 14. Adsorption study with $\alpha_V\beta_3$. This chart follows the growth of the peaks at 1644 cm^{-1} and 1618 cm^{-1}. The trials numbered were consecutive 150 second integration time scans. A neutral point at 1664 cm^{-1} is used to judge the peak height change by way of subtraction of the raw intensities.

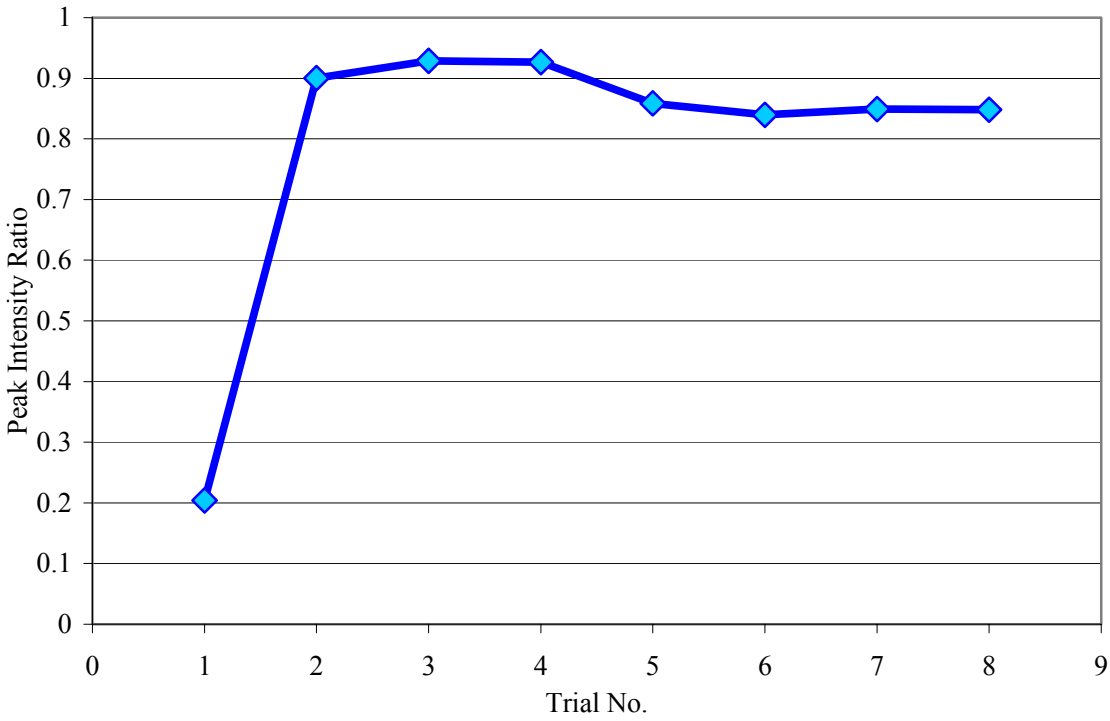

Figure 15. Ratio of 1618.1 cm^{-1} to 1644.8 cm^{-1} peak intensities. After a large jump in the ratio from the first scan to the second the ratio stays fairly constant and that increase of the peak at 1618 cm^{-1} is merely a superposition of the peaks at 1644 cm^{-1} 1618 cm^{-1} and 1569 cm^{-1}.

3.2 INTEGRIN CONCENTRATION STUDY

Once the SERS spectra of both $\alpha_V\beta_3$ and $\alpha_5\beta_1$ had been obtained, the next step was to show the capability to ascertain a concentration dependence trend using SERS. The ability to observe an increase or decrease in the concentration of integrins using SERS would be useful in a combined AFM-SERS system. SERS would be used to detect the change in concentration of the integrins while the AFM is activating the cell surface integrins using a ligand polymerized onto a metal coated AFM tip (Fig 3).

3.2.1 Experimental Method

This procedure is similar to what was done with the adenine concentration studies but with fewer concentrations. The setup for the Raman Spectrometer previously described in section 2.3 was employed. The SERS samples were formed using the same protocol that was previously described using a 10:1:1 ratio of colloid to 1.0 M NaCl to the analyte of interest. The integrin concentrations to be detected were formed at the same time the SERS sample was made up because the integrins had to be stored in undiluted alloquots.

A diluting buffer was made in order to form diluted concentrations of the integrins. The buffer solution that the integrin was shipped in was recreated and used as a diluting agent. The buffer was formed with the following concentrations: 25 mM Tris-HCl, 150 mM NaCl, 1 mM $MgCl_2$, 0.1 mM $CaCl_2$, and 10 mM n-octyl-β-D-glucopyranoside. The n-octyl-β-D-glucopyranoside was obtained from EMD

Biosciences (San Diego, CA) and all other reagents were obtained from Sigma (St. Louis, MO). The pH was adjusted to 7.4 using 1.0 M HCl and 1.0 M NaOH.

The integrins were diluted using the buffer solution to form the desired concentration just before aggregating the colloid. The final integrin concentrations tested using SERS after diluting the integrin and then inserting the dilution into the aggregating colloid were the following: 15 nM, 31 nM, 61 nM, and 122 nM for the $\alpha_V\beta_3$ integrin and 16 nM, 33 nM, 66 nM, and 131 nM for $\alpha_5\beta_1$ integrin.

3.1.2 Results and Discussion

Concentration trends were formed using the two separate integrins $\alpha_V\beta_3$ and $\alpha_5\beta_1$ based on the SERS intensity at four different concentrations. It was only possible to obtain SERS spectra that followed a concentration trend using the citrate reduced colloid because the hydroxylamine hydrochloride reduced colloid was found to be ineffective for SERS enhancement during the first integrin study. As explained in section 3.1.2, the pH of the colloid was not at a level favorable for integrin adsorption. Three spectra showing concentration changes in the $\alpha_5\beta_1$ integrin and two spectra exhibiting a concentration change in $\alpha_V\beta_3$ were obtained (Fig 16 and 17). The three concentrations for $\alpha_5\beta_1$ were 33 nM, 66 nM, and 131 nM, and the two concentrations for $\alpha_V\beta_3$ were 61 nM and 122 nM. The SERS spectra in these concentrations exhibited a majority of the peaks and bands described in the previous spectral analysis section, section 3.1.2. An additional spectrum was obtained of an even lower concentration of $\alpha_5\beta_1$ but the peaks did not lie in the same regions as previously described. The peaks had been shifted and

were not indicative of normal SERS of proteins. It is possible that the minute amount of integrin mixed with a large amount of buffer led to a possible change in silver surface chemistry. Additional salt concentrations that exist in the buffer could have led to a change in how the integrin adsorbs onto the silver surface, thus limiting any SERS from occuring similar to the results of the hydroxylamine hydrochloride reduced colloid [33].

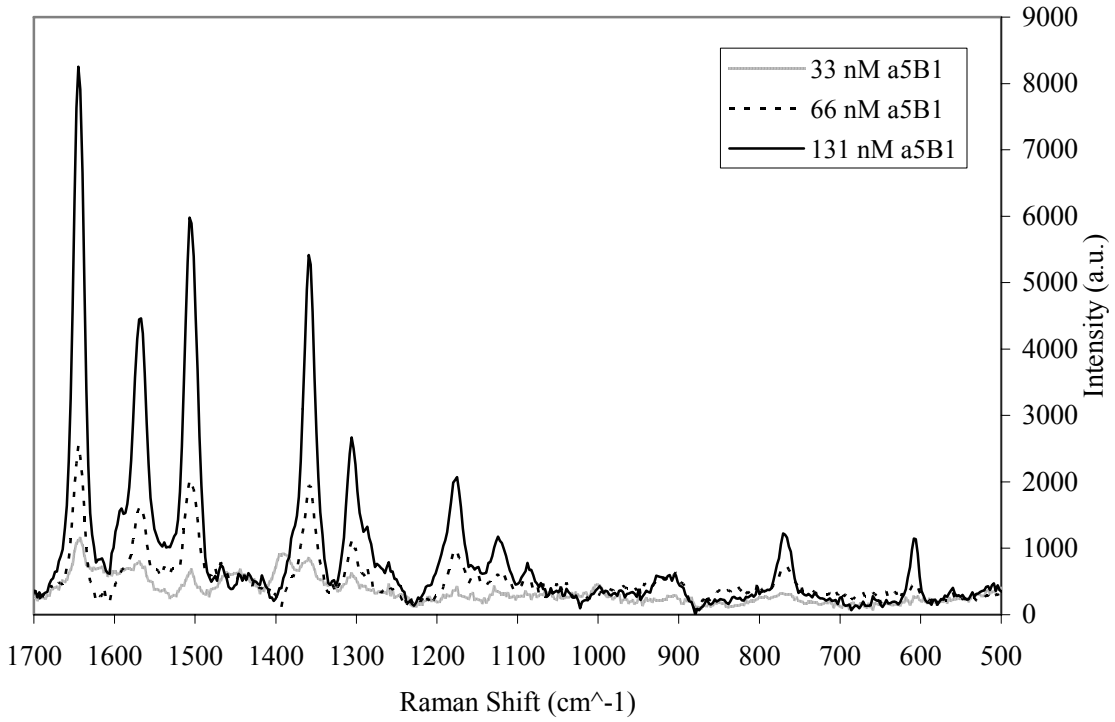

Figure 16. Integrin $\alpha_5\beta_1$ concentration response. SERS spectra were obtained of $\alpha_5\beta_1$ at three concentrations: 33 nM, 66 nM, and 131 nM.

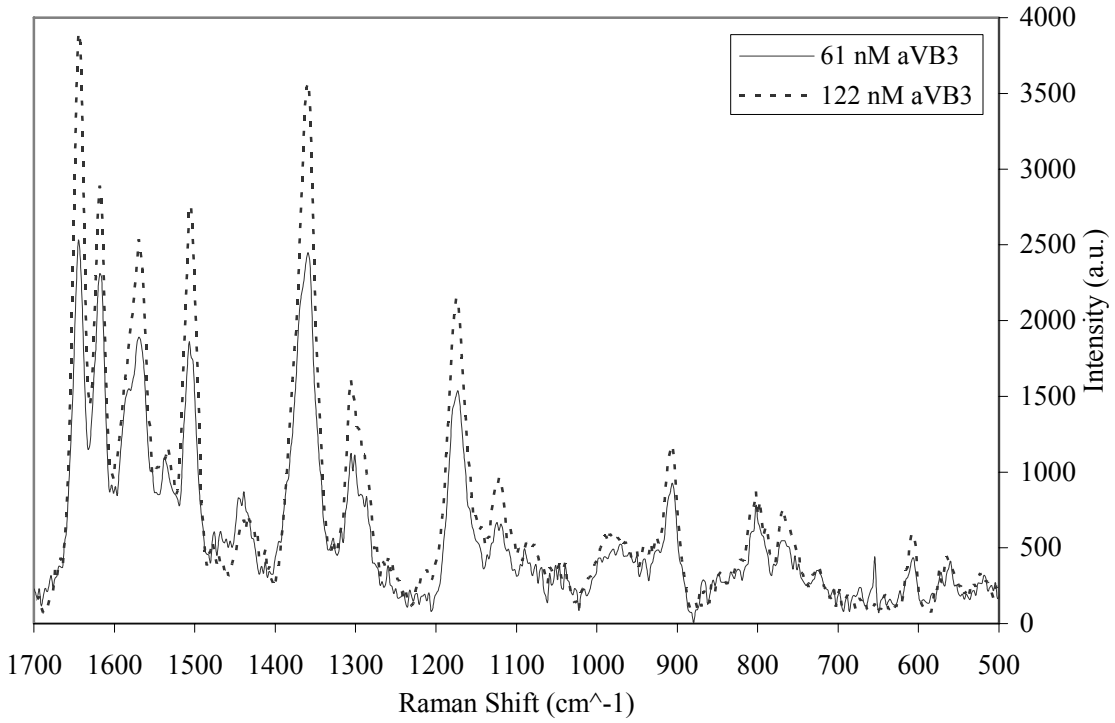

Figure 17. Integrin $\alpha_V\beta_3$ concentration response. SERS spectra were obtained of $\alpha_V\beta_3$ at two concentrations: 61 nM, and 122 nM.

4. CONCLUSIONS AND FUTURE WORK

This thesis has presented evidence that the use of SERS to detect varying concentrations of adenine, integrin $\alpha_V\beta_3$, and integrin $\alpha_5\beta_1$ is possible. All three of the analytes were detected using a citrate reduced silver colloid prepared by a modified Lee and Meisel method [26]. SERS enhancement was observed using a hydroxylamine hydrochloride reduced silver colloid to obtain SERS spectra of adenine as well. The original intent was to obtain SERS spectra using both colloids of all three analytes: adenine, integrin $\alpha_V\beta_3$, and integrin $\alpha_5\beta_1$.

The Leopold and Lendl method of preparing hydroxylamine hydrochloride reduced silver colloids [27] is easier to prepare than the citrate reduced method in terms of the difficulty of the steps involved in the process. The hydroxylamine hydrochloride preparation only involves the addition of two solutions at room temperature and the colloids are immediately ready to use, whereas the citrate reduced colloids require boiling the solution for over an hour before the colloid is ready to be used for SERS. The main purpose of using the second colloid was to determine if the hydroxylamine hydrochloride reduced colloids would be a suitable replacement for the citrate reduced colloid. The results from the SERS spectra of the adenine indicated that the hydroxylamine hydrochloride reduced colloid worked better than the citrate reduced colloid. The secondary peaks in the adenine spectra using the hydroxylamine hydrochloride reduced colloids were more clearly defined than in the spectra formed with the citrate reduced colloids.

In the integrin experiments the hydroxylamine hydrochloride colloid did not show SERS spectra that contained clearly defineble bands indicative of the integrin protein as was shown by the citrate reduced colloid. A pH test after the integrin tests were performed shows that the pH was significantly different between the two colloids. This observation gives rise to the conclusion that poor adsorption of the integrin protein onto the colloid is one reason a well defined SERS spectrum of integrins was not obtained. Furthermore, this implication could also describe why the hydroxylamine hydrochloride reduced colloid outperformed the citrate reduced colloid in the adenine tests.

The observation of a concentration trend using SERS in integrins was thus limited to using the citrate reduced colloid as the source for metal enhancement. However, it was possible to observe a concentration dependence trend of both integrins, $\alpha_V\beta_3$ and $\alpha_5\beta_1$, using the citrate-reduced colloid.

Future experiments should reexamine the use of the hydroxylamine hydrochloride reduced colloid to detect integrins using colloids formed with pH levels close to the levels observed in the citrate reduced colloid. In addition to the pH level experiments, future work should focus on obtaining SERS spectra from a larger range of sample concentrations for the inegrins, as well as detecting other integrins that serve similar functions to the integrins $\alpha_V\beta_3$ and $\alpha_5\beta_1$. These experiments would provide further insight into what would be needed to accomplish the the construction of a combined Atomic Force Microscope with Raman spectrometer system to detect integrins

(Figure 1). This proposed system could then potentially be used to detect the formation of focal adhesions and monitor integrin clustering.

REFERENCES

[1] L.A. Martinez-Lemus, Z. Sun, A. Trache, J.P. Trzciakowski, and G.A. Meininger, "Integrins and Regulation of the Microcirculation: From Arterioles to Molecular Studies Using Atomic Force Microscopy," *Microcirculation*, vol. 12, pp. 99-112, 2005.

[2] I.F. Charo, L. Nannizzi, J.W. Smith, and D.A. Cheresh, "The Vitronectin Receptor $\alpha_v\beta_3$ Binds Fibronectin and Acts in Concert with $\alpha_5\beta_1$ in Promoting Cellular Attachment and Spreading on Fibronectin," *The Journal of Cell Biology*, vol. 111(6), pp. 2795-2800, Dec. 1990.

[3] L.A. Martinez-Lemus, T. Crow, M.J. Davis, and G.A. Meininger. (Feb. 2005) $\alpha_v\beta_3$ and $\alpha_5\beta_1$ Integrin Blockade Inhibit Myogenic Constriction of Skeletal Muscle Resistance Arterioles. *Am. J. Physiol. Heart Circ. Physiol.* [online] Available: http://ajpheart.physiology.org

[4] L.A. Martinez-Lemus, X. Wu, E. Wilson, M.A. Hill, G.E. Davis, M.J. Davis, and G.A. Meininger, "Integrins as Unique Receptors for Vascular Control," *Journal of Vascular Research*, vol. 40, pp. 211-233, 2003.

[5] Y.D. Suh, G.K. Schenter, L.Zhu, and H.P. Lu, "Probing Nanoscale Surface Enhanced Raman-Scattering Fluctuation Dynamics Using Correlated AFM and Confocal Ultramicroscopy," *Ultramicroscopy*, vol. 97, pp. 89-102, 2003.

[6] A.F. Horwitz. "Integrins and Health," *Scientific American*, pp. 68-75, May 1997.

[7] R.O. Hynes, “Integrins: Bidirectional, Allosteric Signaling Machines,” *Cell*, vol. 110, pp. 673-687, 2002.

[8] M.A. Schwartz, M.D. Schaller, and M.H. Ginsberg, “Integrins: Emerging Paradigms of Signal Transduction,” *Cell and Developmental Biology*, vol. 11, pp. 549-599, 1995.

[9] C.K. Miranti and J.S. Brugge, “Sensing the Environment: A Historical Perspective on Integrin Signal Transduction,” *Nature Cell Biology*, vol. 4, pp. 83-90, April 2002.

[10] T. Xiao, J. Takagi, B.S. Coller, J. Wang, and T.A. Springer, “Structural Basis for Allostery in Integrins and Binding to Fibrinogen-mimetic Therapeutics,” *Nature*, vol. 432, pp. 59-67, November 2004.

[11] Y. Chen, T.E. O’Toole, T. Shipley, J. Forsyth, S.E. LaFlamme, K.M. Yamada, S.J. Shattil, and M.H. Ginsberg, “Inside-out Signal Transduction Inhibited by Isolated Integrin Cytoplasmic Domains,” *The Journal of Biological Chemistry*, vol. 269 (28), pp. 18307-18310, July 1994.

[12] R.O. Hynes, “Integrins: Versatility, Modulation, and Signaling in Cell Adhesion,” *Cell*, vol. 69, pp. 11-25, 1992.

[13] F.G. Giancotti and E. Ruoslahti, “Integrin Signaling,” *Science*, vol. 285, pp. 1028-1032, 1999.

[14] E.A. Clark and J.S. Bruggs, “Integrins and Signal Transduction Pathways: The Road Taken,” *Science*, vol. 268, p. 233-239, 1995.

[15] C.V. Raman and K.S. Krishnan, "A New Type of Secondary Radiation," *Nature*, vol. 121, pp. 501-502, 1928.

[16] P.R. Carey, *Biochemical Applications of Raman and Resonance Raman Spectroscopies*. New York: Academic Press, 1982.

[17] C.L. Stevenson and T. Vo-Dinh, "Signal Expressions in Raman Spectroscopy," in *Modern Techniques in Raman Spectroscopy*, J.J. Laserna, Ed. Chichester, England: John Wiley & Sons, 1996, pp. 1-39.

[18] S. Nie and S.R. Emory, "Probing Single Molecules and Single Nanoparticles by Surface-enhanced Raman Spectroscopy," *Science*, vol. 275, pp. 1102-1106, 1997.

[19] S. Stewart and P.M. Fredericks, "Surface-enhanced Raman Spectroscopy of Peptides and Proteins Adsorbed on an Electrochemically Prepared Silver Surface," *Spectrochimica Acta Part A*, vol. 55, pp. 1615-1640, July 1999.

[20] H. Deng, Q. He, Z. Xu, X. Wang, and R. Sheng, "The Study of Turnip Mosaic Virus Coat Protein by Surface Enhanced Raman Spectroscopy," *Spectrochimica Acta Part A*, vol. 49(12), pp. 1709-1714, 1993.

[21] M.J. Weaver, S. Zou, and H.Y.H. Chan, "The New Interfacial Ubiquity of Surface-enhanced Raman Spectroscopy," *Analytical Chemistry*, vol. 72, pp. 38A-47A, 2000.

[22] B. Pettinger, G. Picardi, R. Schuster, and G. Ertl, "Surface-enhanced and STM-tip-enhanced Raman Spectroscopy at Metal Surfaces," *Single Mol.*, vol. 5, pp. 285-294, 2002.

[23] A. Rupérez and J.J. Laserna, "Surface-enhanced Raman Spectroscopy," in *Modern Techniques in Raman Spectroscopy*, J.J. Laserna, Ed. Chichester, England: John Wiley & Sons, 1996, pp. 227-264.

[24] P. Kambhampati, C.M. Child, M.C. Foster, and A. Campion, "On the Chemical Mechanism of Surface Enhanced Raman Scattering: Experiment and Theory," *Journal of Chemical Physics*, vol. 108 (12), pp. 5013-5026, March 1998.

[25] D.H. Everett and L.K. Koopal, (2001) *Definitions, Terminology and Symbols in Colloid and Surface Chemistry, Part I*. (Internet Edition) [Online]. Available: http://www.iupac.org/reports/1972/3104everett/

[26] P.C. Lee and D. Meisel, "Adsorption and Surface-Enhanced Raman of Dyes on Silver and Gold Sols," *J. Phys. Chem*., vol. 86, pp. 3391-3395, 1982.

[27] N. Leopold and B. Lendl, "A New Method for Fast Preparation of Highly Surface-Enhanced Raman Scattering (SERS) Active Silver Colloids at Room Temperature by Reduction of Silver Nitrate with Hydroxylamine Hydrochloride," *J. Phys. Chem. B*., vol. 107, pp. 5723-5727, 2003.

[28] K. Kneipp, H. Kneipp, V.B. Kartha, R. Manoharan, G. Deinum, I. Itzkan, R.R. Dasari, and M.S. Feld, "Detection and Identification of a Single DNA Base Molecule Using Surface-enhanced Raman Scattering (SERS)," *Phys. Rev. E*, vol. 57, pp. R6281, 1998.

[29] G. Mie, "*Beitrage Zur Optic Truber Medien, Speziell Kolloidaler Metallosungen*," *Ann. Physik*, vol. 25, pp. 377-445, 1908.

[30] J.E. Mogford, G.E. Davis, S.H. Platts, and G.A. Meininger, "Vascular Smooth Muscle Alpha V Beta 3 Integrin Mediates Arteriolar Vasodilation in Response to RGD Peptides," *Circ. Res*., vol. 79, pp. 821-826, 1996.

[31] J.E. Mogford, G.E. Davis, and G.A. Meininger, "RGDN Peptide Interaction with Endothelial $\alpha_5\beta_1$ Integrin Causes Sustained Endothelin-dependent Vasoconstriction of Rat Skeletal Muscle Arterioles," *J. Clin. Invest*., vol. 100, pp. 1647-1653, 1997.

[32] V.M. Belkin, A.M. Belkin, and V.E. Koteliansky, "Human Smooth Muscle VLA-1 Integrin: Purification, Subtrate Specificity, Localization in Aorta, and Expression during Development," *The Journal of Cell Biology*, vol. 111, pp. 2159-2170, November 1990.

[33] J. Hu, R.S. Sheng, Z.S. Xu, and Y. Zeng, "Surface Enhanced Raman Spectroscopy of Lysozyme," *Spectrochimica Acta Part A*, vol. 51(6), pp. 1087-1096, 1995.

[34] Z.Q. Wen, S.A. Overman, P. Bondre, and G.J Thomas, Jr., "Structure and Organization of Bacteriophage Pf3 Probed by Raman and Ultraviolet Resonance Raman Spectroscopy," *Biochemistry*, vol. 40, pp. 449-458, Jan. 2001.

VITA

Virgil Alexander Gant was born on April 21, 1980 in Galveston, Texas. In August of 2002, he received his Bachelor of Science degree in Biomedical Engineering from Texas A&M University. His research was focused on surface enhanced Raman spectroscopy. He intends to attend medical school after receiving his Master of Science degree in Biomedical Engineering. He can be contacted through email at alex.gant@gmail.com. He can also be reached by mail at 2102 Limrick Drive, Pearland, TX, 77581.

The typist for this thesis was Virgil Alexander Gant.